Development of a CRISPR/Cas9 mutation system in *Caenorhabditis briggsae* and use in altering the Notch signaling pathway

Undergraduate Research Thesis

Presented in Partial Fulfillment of the Requirements for graduation "with Honors Research Distinction in Molecular Genetics" in the undergraduate colleges of The Ohio State University

by
Robert Smith

The Ohio State University
April 2017

Project Advisor: Professor Helen Chamberlin, Department of Molecular Genetics

Introduction

The cell signaling pathways mediated by Notch and Epidermal Growth Factor (EGF) are critical pathways found across the entire animal kingdom (Artavanis-Tsakonas et al., 1999). Mutations and errors causing disruptions in these two pathways have been connected with a variety of cancers (Galluzzo and Bocchetta, 2011). Depending on the tissue type, the same Notch and EGF components can function either as oncogenes or tumor suppressors (Espinoza and Miele, 2013). To better understand the functioning of the two pathways and the manner in which they interact, research on basic model organisms like the nematode is needed. This can provide insight into the differential functioning of the two pathways based on cellular background.

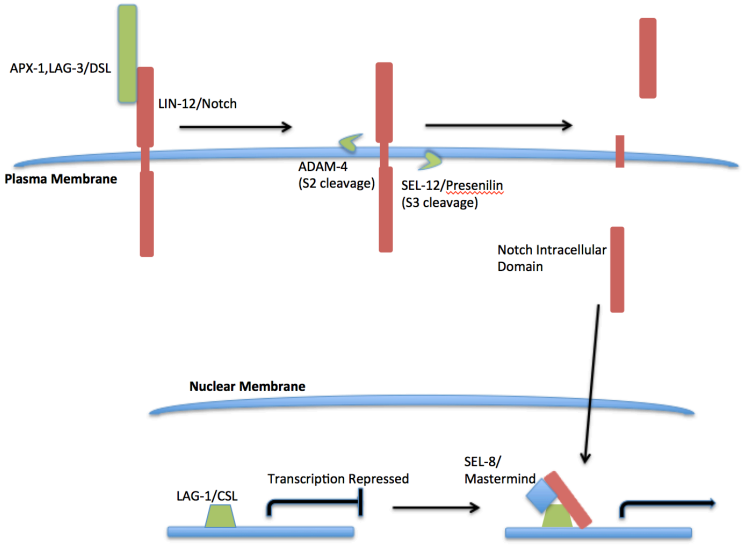

Figure 1: Diagram of typical Notch signal transduction in nematodes

The Notch signal transduction pathway operates through a ligand/receptor interaction between two cells. In nematodes, the "DSL" ligand of LAG-2 or APX-1 released by one cell will interact with the LIN-12 transmembrane receptor on the target cell to cause a cleavage of the extracellular domain. This will lead to a further cleavage of LIN-12 in the transmembrane portion that leads to its release. The intracellular portion will then drop into the nucleus and form a complex with SEL-8 and LAG-1. Normally, LAG-1 acts as a repressor of the target gene but the formation of the complex allows it to induce DNA transcription (Petcherski and Kimble, 2000). In nematodes, EGF signaling involves the ligand LIN-3 binding to a receptor tyrosine kinase such as LET-23 which leads to the activation of the RAS ortholog LET-60. This causes a phosphorylation cascade and transcription of a target gene through transcription factors such as LIN-31 (Yamamoto et al., 2014). The EGF and Notch pathway have been shown to cooperate and antagonize each other in nematodes as well as in other species. During the development of the *Drosophila* eye, high Notch activity and low EGF levels are both required for early photoreceptors to progress past the G1 phase and continue dividing (Baker and Yu, 2001). In the same environment the two pathways also work together to stimulate cone cell formation. Both are needed at high levels to promote specific transcription factor activity (Flores et al., 2000). Notch and EGF have been shown to antagonize each other in the *Drosophila* eye, as well as in species like the zebrafish where Ras-activated factors will antagonize Notch-induced factors if both are present (Kawamura et al., 2005). Additionally, microarray-based transcriptome analysis in *Drosophila* has

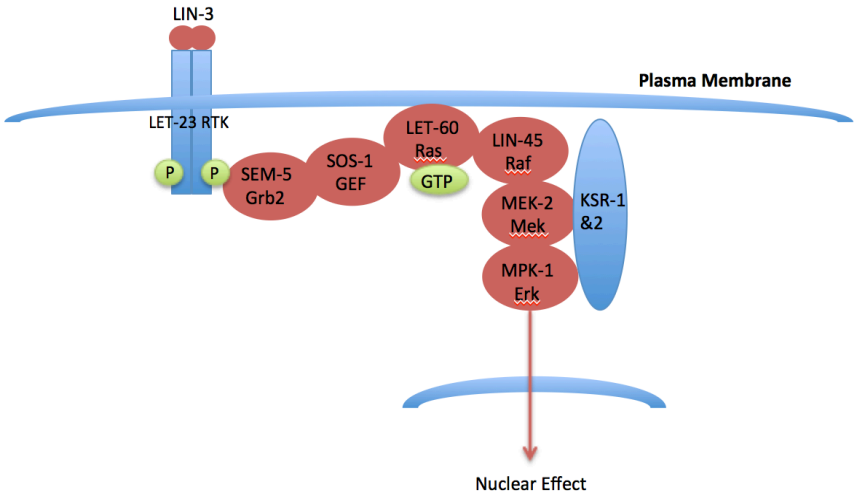

Figure 2: Diagram of EGF signal transduction in nematodes.

shown that 65% of transcriptional targets are shared between the two pathways (Guruharsha et al., 2012). This project focused on the nematode vulva, and both signaling pathways must interact in the proper way in order to let the vulva form correctly. However, this experiment dealt with disruption of the Notch pathway to observe effects on vulval development.

Caenorhabditis elegans and *Caenorhabditis briggsae* were the subjects used in this project. Both are nematodes that have their genomes sequenced and mapped; in the case of *elegans* the entire cell lineage determined (Giurumescu and Chisholm, 2011). The two species diverged from each other about 30 million years ago, yet about 62% of genes have a direct ortholog found in the other (Gupta and Sternberg, 2003; Cutter, 2008). Both species have a similar genome size (102 Mb for *elegans* and 104 Mb for *briggsae*) and six chromosomes. Additionally, the development of the vulva is conserved and occurs in a very similar way at a cellular level (Horvitz and Sternberg, 1991).

Despite the large amount of genes without a direct ortholog found between the two species, *elegans* and *briggsae* are near identical in respect to morphology and behavior. One area where the two differ greatly is in vulva formation. While normal vulval development is identical in the two species in cells, experimental results argue that both exhibit biochemical differences in the way precursor cells signal to each other during the vulva's growth (Dawes et al., 2017).

During the formation of the nematode vulva, six vulval precursor cells (VPCs) located in the ventral epidermis of the worm are stimulated by another cell called the anchor cell located just dorsal to the six (Sherwood and Sternberg, 2003). In *C. elegans,* during the L3 larval stage, the anchor cell will release the EGF signal through LIN-3 and cause the nearest VPC (P6.p) to adopt the primary cell fate and become the apex of the vulva. The two cells adjacent to P6.p will take on a

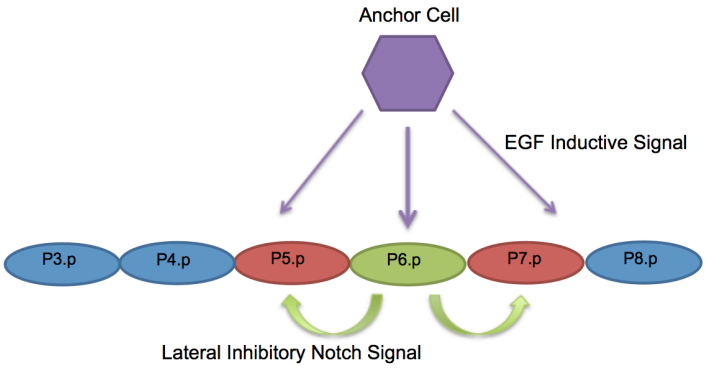

Figure 3: Initial signaling in the development of the vulva

secondary cell fate to form the sides of the vulva and the other three VPCs will all adopt a non-specialized tertiary fate causing fusion with the epidermal syncitium (Wang and Sternberg, 2001). Figure 3 gives a graphical representation of the process.

In both these species, current literature indicates that the specification of the primary and secondary fate in VPCs comes from a combination of sequential and morphogen-based induction. The primary cell fate is determined by proximity to the anchor cell EGF signal and amount of signal received (Herman and Hedgecock, 1990). Secondary cell fates are derived from a combination of a weaker EGF signal and an inhibitory signal from the primary cell through the Notch pathway (Berset et al., 2001). Experiments involving ablation of the anchor cell early in nematode development always leads to a vulvaless phenotype in both *C. elegans* and *C. briggsae* (Félix 2012). In *C. elegans,* the adoption of the primary fate by P6.p is especially dependent on the EGF signal; later in vulval development, *C. elegans* VPCs will remain undivided and unspecialized if the EGF anchor cell signal is eliminated through the application of a U0126 MEK inhibitor that removes signaling from the EGF pathway (Dawes et al., 2017). Conversely, *C. briggsae* nematodes will have VPCs P5.p-P7.p adopt secondary cell fates when the U0126 is applied, indicating sensitivity in the absence of the anchor cell EGF signal. (Dawes et al., 2017). This indicates a major difference between the two species in how the EGF signaling pathway patterns the VPCs. *C. briggsae* nematodes may retain vulval competence through a variety of ways: an additional signal from the anchor cell, signals from other surrounding cells, or a Notch signal coming internally from P5.p-P7.p. *C. elegans* nematodes express a *Cel-lip-1::GFP* transgene (indicative of Notch signaling) only in P5.p and P7.p, the cells that typically assume a secondary fate (Félix 2012). *C. briggsae* nematodes express the same reporter in P5.p-P7.p normally, suggesting that Notch may have a strong role in providing VPC competence in *C. briggsae* (Félix 2012).

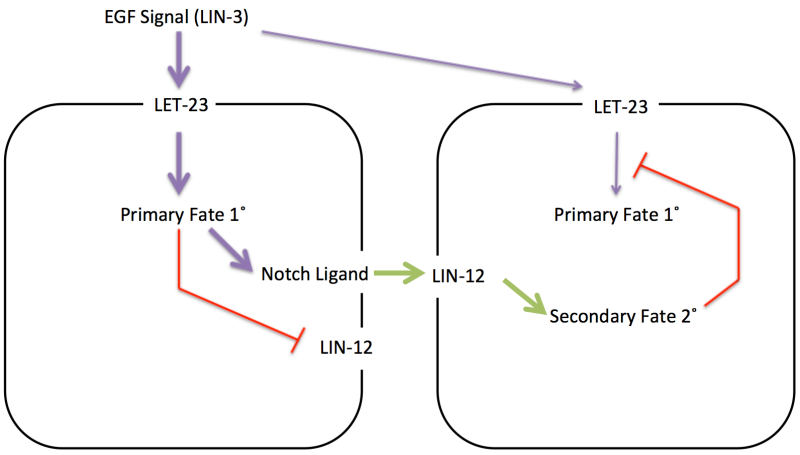

Figure 4: Proposed model of Notch-EGF interaction in specifying VPC fate

The goal of this project was to further analyze this variation by studying the effects of Notch mutations in *C. briggase*. By hyperactivating and destroying the function of the LIN-12 receptor, this experiment hoped to show the effects of a constitutively active Notch pathway and a nonexistent pathway. If worms with these mutations were obtained, MEK inhibitor U0126 would be applied to the worms to then see the effect of EGF signaling removal. With *C. briggsae*, it was

predicted that overexpressing Notch would lead to VPCs overpowering the EGF signal and all adopting a secondary fate; on the contrary, a lack of Notch signaling would allow an EGF-driven primary fate to be taken on by all the VPCs. U0126 would likely have no effect on constitutive Notch worms and would probably create a vulvaless phenotype in worms without a Notch signal.

To generate the desired mutations, this project sought to apply uniquely devised Co-CRISPR strategies to induce the desired mutations in *C. briggsae* nematodes. A clustered regularly interspersed short palindromic repeats (CRISPR)-Cas9 system allows the targeting of a specific gene and the ability to place a specific mutation or indel in the gene (Ma et al., 2014). The system uses a Cas9 protein, normally involved in bacterial defense systems against viruses, to cut at a particular point indicated by a CRISPR RNA. This model has been adapted for use in *C. elegans* and has shown promising signs of effectiveness (Paix et al., 2015). To induce a mutation, a single guide RNA (sgRNA) must be created first. This is a singular large strand of RNA that contains a tracrRNA that binds the Cas9 protein and the CRISPR RNA (Zhang et al., 2014). The sgRNA needs to contain a 20 base pair guide sequence at the 5' end which pairs with the target DNA and directs the Cas9 protein to cleave at a certain sequence. Aside from the guide sequence, Cas9 also requires a three base pair protospacer-adjacent motif (PAM) located next to the guide sequence that allows Cas9 to bind (Zhang et al., 2014). In this experiment, a Cas9 protein was used that requires a PAM of NGG.

Co-CRISPR requires the creation of two sgRNA plasmids: one that contains an sgRNA targeting a gene with a known effect and an sgRNA containing the mutation of interest. It allows a mutation with unknown effects to be readily identified in nematodes by association with another successful and known mutation (Arribere et al., 2014). This saves large amounts of time in post-injection PCR screening. A worm showing the effects of the known sgRNA mutation likely has the unknown sgRNA expressed as well. In CRISPR the primary reason causing a cloned plasmid to not express is the lack of active Cas9 machinery in the oocyte. Often, as long as the cell contains active Cas9, both sgRNAs on their respective plasmids will be expressed (Kim et al., 2014).

This project used marker alleles of genes that had previously been characterized: *Cel-rol-6 (su1006), Cel-dpy-10 (cn64), and Cel-sqt-1(e1350)*. These alleles were shown to be easily phenotypically identifiable in a Cas9 system and lead to the isolation of affected nematodes in only a few generations (Arribere et al., 2014). Each gene codes for a cuticle collagen, and a change from an arginine to cysteine in each case leads the mutation in *rol-6* and *sqt-1* to create right rollers and the allele in *dpy-10* to cause left rollers (Arribere et al., 2014). All of these alleles caused dominant mutations as well leading to easier screening. In addition, the mutant phenotypes were distinct from null mutations, meaning candidate rollers had undergone a CRISPR repair through homology directed repair, rather than an indel caused by non-homologous end-joining. Previous work on the alleles was all performed in *C. elegans*, so the associated sgRNA and oligonucleotide repair templates had to be reproduced using the *C. briggsae* genome. Fortunately, the two species are related enough that the specific mutation found for each allele could still be nearly exactly replicated in *C. briggsae*.

Materials and Methods

Strains

The Bristol N2 strain was used in experiments performed on *C. elegans* and the strain AF16 was used for all experiments involving *C. briggsae*. Both were grown on nematode growth medium (NGM) in plates containing OP50 bacteria (Brenner 1974).

CRISPR Methodology

As described, CRISPR requires the use of sgRNAs, an expressed Cas9 protein, and donor repair template. For transformation, a single-stranded oligonucleotide or donor plasmid containing a repair template is required; this experiment used the oligonucleotide. This experiment used short-range homology directed repair to create point mutations to cause a desired phenotype. An ideal repair template needed to be less than approximately 100 base pairs (Dickinson et al., 2013). After Cas9 cleaves the DNA at the cut site, the blunt ends are trimmed back and then allow the donor oligonucleotide to begin repair based off of the homologous region. Once successfully cloned, the modified pDD162 was injected into worms along with a GFP marker. The plasmid pDD162 contains the Cas9 coding sequence attached to the gene *eef-1A's* promoter and the sgRNA attached to a universal U6 promoter allowing expression through RNA polymerase III (Dickinson et al., 2013). Follow-up evaluation was then performed on worms manifesting the desired phenotype.

sgRNA Creation

For each Co-CRISPR marker gene, the genome location of the *C. elegans* mutation was first identified in the *C. briggsae* genome. The species are close enough that the same mutations could be applied to *C. briggsae*. Next, suitable sgRNAs were found using the site http://crispr.mit.edu (Hsu et al., 2013). The site provides all possible guide sequences found within a range of the data inputted and provides statistics on each comparing the specificity and likelihood of effectiveness. The tool was only able to compare against the *C. elegans* genome, so after selection of an sgRNA each was compared against the *C. briggsae* genome to ensure no unexpected matches in other genes. Thus sgRNAs were found for *Cbr-rol-1, Cbr-dpy-10, Cbr-sqt-1,* a predicted constitutive dominant mutation in *Cbr-lin-12,* and a predicted loss-of-function mutation in *Cbr-lin-12* (Figure 5). After ordering, each sgRNA was placed into the pDD162 plasmid. The type of Cas9 used in these experiments requires a guanine before the 20 base pair guide sequence. After the promoter, pDD162 contains this guanine and is the optimal plasmid for the strain of Cas9 used. Cloning into the plasmid began with overlap extension PCR, where varying concentrations of marker sgRNA oligonucleotides were used in the PCR (10 ng/µl and 40 ng/µl) since these were shown to previously be the optimal concentrations (Arribere et al., 2014). Afterward, DpnI was used to digest away any original methylated plasmids and then followed up with a ligation to attach the blunt ends. Plasmids were then used to transform DH5α *E. coli* bacteria and positively selected for through carbenicillin agar plates. Experimental results were compared against control

plates that contained plasmids that underwent the initial PCR without a DNA extension enzyme. Experimental plates that showed significantly more colonies than control plates had colonies cultured and plasmids extracted for further evaluation. Potential colonies were cultured and plasmids were recovered for verification PCR using specific primers flanking the mutation site of interest. PCR amplified segments were tested through a restriction enzyme digest and any plasmids with positive results were sequenced to ensure the presence of the sgRNA insert.

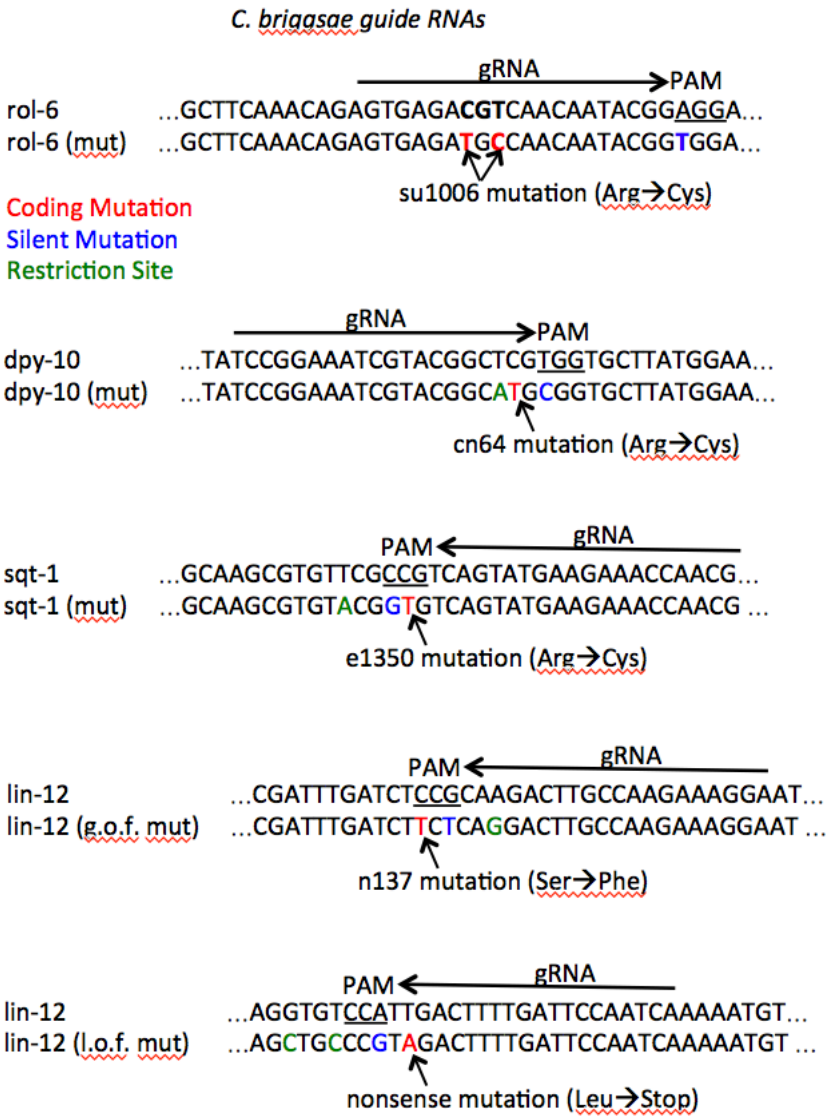

Figure 5: *C. briggsae* sgRNAs developed for all markers and Notch

Repair Oligonucleotide Creation

The desired mutations for each sgRNA to create were all point mutations; therefore, the repair oligonucleotides were made at the maximum length that would still be repaired using the highly efficient short-range homology directed repair (100 bp). Aside from the point mutation to alter phenotype, two other changes had to be incorporated into each oligonucleotide: ones changing the PAM site/multiple points in the cut site to prevent repeated Cas9 cleavage and additional ones to create a novel restriction enzyme cut site for easier screening. Figure 5 includes the modified parts of the repair template.

Verification of introduction of DNA Changes

In order to determine if DNA changes had properly been installed into the nematode genome, verification primers and sequencing primers were designed as well. The designed repair templates had alterations placed in them that would create a restriction enzyme cut site around the experimental point mutation. These verification primers amplified a region in the DNA ~250 base pairs away on either

side of the point mutation. When cut with the restriction enzyme, the repaired DNA would present at different sizes than wild type DNA because of the added (or deleted) cut site. Additionally, sequencing primers that could read internal to the verification primers were also created to completely verify presence of the repair template insertion. Specific sequences of primers are found in S3 and S4.

Injections

DNA was injected into the germline of wild-type animals (*C. elegans* or *C. briggsae*) following standard protocols (Mello et al., 1991). For every individual marker sgRNA designed, an initial injection was performed containing sgRNA at a concentration of 50 ng/µl, repair oligonucleotide at 20 ng/µl, and a *myo-2* GFP marker at 25 ng/µl. The GFP marker was present to identify successful injection of the mix into the nematode gonad. For Co-CRISPR, the same concentrations were used for marker sgRNA, repair oligonucleotide, and *myo-2* GFP marker except another dose of experimental sgRNA and repair template was added. In these mixes, the final concentration of DNA present in the injection mixture was 165 ng/µl.

Screening

F1 worms that exhibited the dominant co-CRISPR phenotype (e.g., Rol) were selected to individual plates and allowed to self-cross. After allowing about 1 week for these individual nematodes to produce a subsequent generation and clear the bacteria from the plate, worms were then harvested through an M9 washing procedure, and frozen at -80C. DNA was recovered by adding worm lysis buffer containing proteinase K at a concentration of 10 ng/mL and then incubating the tube at 60˚C for one hour and then inactivated the reaction enzyme through a fifteen minute 95˚C heating period. Afterward, the extracted experimental DNA was put through PCR along with a positive control wild-type DNA. Amplified DNA was digested with their respective restriction enzymes for four hours along with undigested controls and run on a 2% agarose gel for size comparison. Any experimental sample that displayed at the correct expected size was further purified using the PCR nucleic acid purification kit and then put in for sequencing using the gene's respective sequencing primer.

Results

Verification of the co-CRISPR method using C. elegans

Before any of the *C. briggsae* CRISPR plasmids were designed, *C. elegans* Cas9 systems were tested to see the efficacy of Cas9 in nematodes firsthand. Identical sgRNAs, repair templates, verification primers, and sequencing primers from the paper Arribere 2014 were cloned into pDD162 and injected into worms (Figure S1, S2, S3, S4). All candidate marker gene, *rol-6, dpy-10, and sqt-1*, were put through an overlap extension PCR, ligation, and transformation process similar to that described in the methods. Fragments were then digested using a specific enzyme that showed varying results depending on successful insertion of the sgRNA. Successful results were indicated by gels that cut at expected sizes against wild type

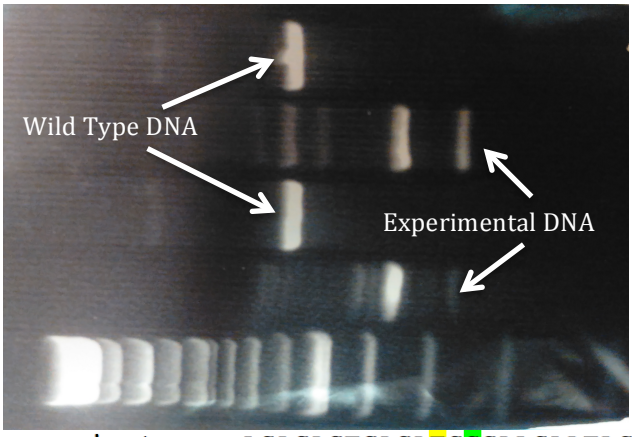


```
repair temp.  ACAGAGTGAGATGCCAACAATACGGTGGATAC
screen 1      ACAGAGTGAGATGCCAACAATACGGTGGATAC
screen 2      ACAGAGTGAGATGCCAACAATACGGTGGATAC
screen 3      ACAGAAATAGAT---AACAATA-----GAACT
```

Figure 6: (top) Gel showing evidence of successful *dpy*-10 repair template incorporation into N2 nematodes. Wild type expected cut size was 631 base pairs and 368 and 263 pairs for mutant (bottom) Example of sequencing results from candidate *dpy-10* mutated N2 nematodes. Screens 1 and 2 indicate success of transformation and 3 is a case of failed cutting.

genomic controls. In *elegans*, expected positive gel results were obtained for *rol-6* and *dpy-10*. *Sqt-1* never displayed a significantly greater amount of colonies when compared to the control so it was not further analyzed as a candidate. Each marker gene was individually injected into *elegans* worms evaluate their effectiveness. F1 worms were self-crossed and the progeny's DNA was harvested after one week. DNA was extracted and checked for mutants after this through sequencing. Often, negative results would not display a wild-type conformation, but a deletion around the site of interest or unexpected mutation (Figure 7). It is possible that Cas9 did cut in these cases but the repair template was not used in repair, leaving the cell to use nonhomologous end-joining to repair the double-stranded break. Another option is that the repair oligonucleotide may not have been present in the cell and segregated independently of the sgRNA-containing plasmid. Regardless, *C. elegans rol-6* and *dpy-10* marker genes were shown to be competent for further analysis using Co-CRISPR.

Development of a co-CRISPR method for *C. briggsae*

For the *C. briggsae* Cas9 systems, the marker gene mutations injected into the nematodes also had success (materials listed in S1, S2, S3, and S4). The best results came from the *Cbr-rol-6* marker. First generation rollers were found to be heterozygous for the experimental repair template and manifested the expected right-rolling phenotype. These results were verified

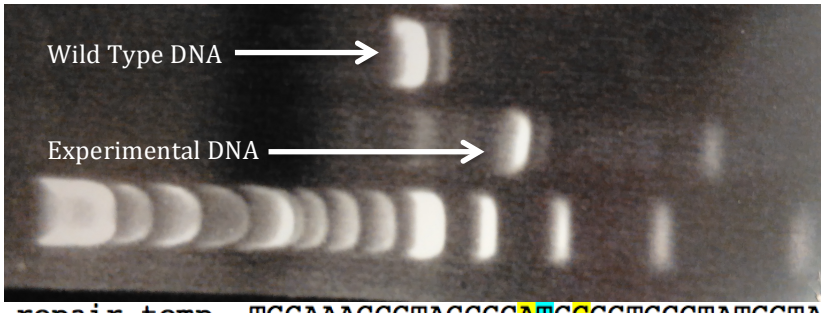


```
repair temp.  TGGAAACCGTACCGCATGCGGTGCCTATGGTA
screen 1      TGGAAACCGTACCGCATGCGGTGCCTATGGTA
screen 2      TGGAAACCGTACCGCATGCGGTGCCTATGGTA
screen 3      TGGAAACCGTACCGCNCGNGGTGCCTATGGTA
```

Figure 7: (top) Gel evidence of *rol-6* transformation of AF16 *briggsae* nematodes. Wild type expected cut size was 528 base pairs and 373and 155 pairs for mutant (bottom) Sequencing results showing successful mutation of worms. Screens 1 and 2 indicate perfect repairs and screen 3 a case of aberrant CRISPR repair.

through restriction digests and sequencing (Figure 7). The other marker genes *dpy-10* and *sqt-1* had similar issues to the *elegans* markers; some candidates contained nonsense inserts around the cut site or simply had a portion of the targeted area deleted. Despite the success with single marker injection, nematodes co-injected with either *lin-12* gain or loss of function sgRNAs and repair templates as well as a *Cbr-rol*-6 marker failed to display any phenotype that was detectable through microscopy and any candidates genotyped did not contain the experimental repair template in the genome (Figure 8).

	rol-6 phenotype	*lin-12* loss evidence	*lin-12* g.o.f. evidence
lin-12 co-CRISPR injection success rate	9/9 (100%)	0/4 (0%)	0/5 (0%)

Figure 8: Five nematodes from *Cbr-lin-12* g.o.f. and *Cbr-rol-6* co-injections displayed the rolling marker phenotype and had lines made from them for further evaluation. Four *Cbr-lin-12* l.o.f. co-injections were examined as well but no evidence of *lin-12* mutant phenotypes was confirmed.

Discussion

Development of a co-CRISPR method for *C. briggsae*

The *C. elegans* plasmids used in this experiment where already designed and investigated by a previous study (Arribere et al., 2014) but were shown to be highly effective as Co-CRISPR markers when injected firsthand. Markers in *C. briggsae* were not as successful, but *Cbr-rol-6* was still found to be a useful marker. Although the *lin-12* experiments are to this point unsuccessful, this plasmid can still be used for many other Co-CRISPR experiments to aid in identifying unknown phenotypes. Additional markers can sill be tested in *C. briggsae*, many genes leading to an uncoordinated phenotype have potential as markers as well.

Possible Causes of *lin-12* negative Results

For *lin-12* mutations the lack of results could have stemmed from a multitude of issues. First, the previously described cases could have occurred where Cas9 fails to cut properly or the CRISPR materials for the experimental *lin-12* alterations failed to segregate to the same oocyte as the marker gene CRISPR materials. Previous studies applying CRISPR to *C. elegans* have reported varying rates of success ranging from 1-16% of F1 progeny showing successful HDR mutation (Dickinson et al., 2013; Arribere et al., 2014; Kim et al., 2013). The dearth of *lin-12* candidates may arise from too little screening. At this point, there is some luck involved in the CRISPR process, and so far injections and screening may have simply not provided any successful candidates. Co-CRISPR undeniably increases the rate of detection of cutting events when searching for NHEJ events, but it is not as effective when searching for HDR events (Kim et al., 2013). The Cas9-sgRNA complexes are assembled in the germline cytoplasm. After this, the CRISPR machinery may be

placed into oocytes independently of the repair templates. Cas9 also has a relatively high tolerance for mismatches. Studies have found that this endonuclease can still cut at a site containing as many as six mismatches in the cut site (Jinek et al., 2012). Despite induced mutations in the cut sites and PAM sequences, there is still a chance that Cas9 has been cutting off target and altering the genome in irreparable ways. To add to this, the briggsae genome is sometimes not fully annotated and constructed. Even though each guide RNA sequence was tested against the genome using BLAST, sites that are not fully put together could have matched to the guide and allowed off target cuts.

Additional explanations include issues with the markers and guide RNAs used. The *rol*-6 marker had previously been tested in *C. elegans* and had shown success firsthand in this lab, but still remains somewhat unknown in *C. briggsae.* Other studies using Co-CRISPR call for a marker that has an intermediate amount of effectiveness. A marker that works too well could show a large proportion of false positives where the marker is successful while the experimental CRISPR is not. Conversely, a marker that is too ineffective might show very randomly and again not be a good indicator for *lin-12* mutations, since the marker would rarely show itself (Kane et al., 2016). For Cas9, the optimal guide RNA contains a dual guanine site previous to the PAM (Dickinson et al., 2013). In the case of the *lin-12* gain of function sgRNA designed, these guanines were not present. A better sgRNA that does contain this could potentially increase the rate of cutting. Finally, the concentration of pDD162 injected may have an effect on the efficiency. The plasmid was injected at 10 ng/mL and 40 ng/mL, both of which were shown to have high success previously (Dickinson et al., 2013). Other concentrations could be tried to find the optimal condition.

For the *lin-12* gain of function allele, the *n137* mutation has been highly characterized in *C. elegans* and is known to cause a constitutively expressing Notch pathway through alteration of the LIN-12 receptor (Greenwald and Seydoux, 1990). The mutation involves a missense point mutation to create the effect. In *C. briggsae*, it is hypothetically possible to induce the same effect using the same mutation since the sequence around the point of interest are directly orthologous between *C. elegans* and *C. briggsae* for hundreds of base pairs; however, this mutation has not been as well defined in *briggsae* and may not have the same effect. Similarly, the attempted loss of function alteration was a completely novel nonsense mutation that had not been characterized in *elegans* or *briggsae*. The change would have ideally truncated the LIN-12 protein severely and prevented transmission of any signal. Additional issues regarding functional differences in *lin-12* between the species might have prevented the manifestation of any mutant phenotype. *C. briggsae* contains a highly identical paralog to *lin-12* (96% identical at the nucleotide level) that could have evaded conversion by the loss of function repair template and compensate for the loss of the initially targeted paralog (Rudel and Kimble, 2002). However, PCR screening would have likely still detected mutant alleles in nematodes displaying no phenotype.

A final reason that could point to lack of experimental *lin-12* candidates could be the promoters used to express the sgRNA and the Cas9 protein. Plasmids utilizing *C. elegans* promoters driving expression of sgRNA and Cas9 were used for

the *C. briggsae* studies. The U6 and *eft-3* promoter are expressed practically universally in the nematode, but it is not known if there might be differences between the *C. elegans* and the *C. briggsae* promoters. In *C. elegans,* a *lin-12* paralog, *glp-1,* is able to take over the function of *lin-12* in all cells of the worm except those involved in the formation of the vulva (Lambie and Kimble, 1991). The relationship between *glp-1* and *lin-12* is less defined in *briggsae,* but total loss of *lin-12* does lead to larval lethality (Rudel and Kimble, 2002). The two promoters used may have overexpressed and underexpressed *lin-12* throughout the entire nematode and thus led to lethality.

Future Experimental Changes

Two aspects of the CRISPR techniques used stand out as candidates for experimental alterations: the plasmid and guide RNA chosen as well as the types of mutation aimed for with *lin-12*.

The pDD162 plasmid is effective in CRISPR in *elegans,* but may not be as useful in *briggsae* due to the promoters that it contains. The U6 and *eft-3* promoter are both derived from *C. elegans*. A possible solution might come from cloning in promoters more specific to *C. briggsae* (either from orthologous or novel genes). Another possible change could come from more specific guide RNAs for the *lin-12* sequences that contain guanines prior to the PAM sequence.

One other possibility for increasing efficiency could come from changing the Cas9 endonuclease so that it operates as a nickase. Normally, Cas9 contains two nuclease domains that cleave the complementary and non-complementary DNA site (Jinek et al., 2012). If this occurs then the DNA will be repaired by the highly efficient base excision repair system (Dianov and Hubscher, 2013). If a repair template is provided, then HDR has been shown to be preferred over NHEJ (Cong et al., 2013). This method would require the development of two plasmids that would both have to segregate to the same oocyte. As prior mentioned, this already can be a reason for low cutting efficiency.

Finally, the *lin-12* mutations themselves could be changed. The desired gain of function mutation simply may not create the same effect in *C. briggsae* that is seen in *C. elegans*. Other comparable and characterized mutations identified in *C. elegans* could be tried in *C. briggsae* as n137 was, but there is still no guarantee of success. As for the loss of function mutation, the goal of a nonsense point mutation may be simplified by aiming for NHEJ repair after cutting. This type of repair has a higher success rate (Dickinson et al., 2013) and would still destroy the gene if used to fix the double-stranded break.

Supplementary Data

Experimental sgRNAs (S1)

Single-guide RNAs contained an NGG PAM site and optimally had a guanine before the PAM site. All marker sgRNAs had at least a 3 base pair difference between the target sequence and any other genome locus. Each sgRNA also included the desired restriction enzyme cut site. Highlighted text indicates a PAM site.

Cel-rol-6
GTGAGACGTCAACAATATGG AGG

Cel-dpy-10
GCTACCATAGGCACCACGAG CGG

Cel-sqt-1
ATGTGGAGTTGGGGTAGCGT TGG (forward)
TGGAAGGACATAGTTGTCAT CGG (reverse)

Cbr-rol-6
GTGAGACGTCAACAATACGGAGG

Cbr-dpy-10
TCCGGAAATCGTACGGCTCGTGG

Cbr-sqt-1
CGTTGGTTTCTTCATACTGACGG

Cbr-lin-12 constitutive
TCCTTTCTTGGCAAGTCTTGCGG

Cbr-lin-12 l.o.f
TGATTGGAATCAAAAGTCAATGG

The constitutive mutation was based off the *n137* allele found in *C. elegans*. This is a missense mutation that manifests a very strong gain of function phenotype. The *C. briggsae* genome matched the *C. elegans* exon exactly around the point mutation so this was used as the basis for its creation. The loss of function sgRNA was an induced nonsense mutation in exon 2 of *lin-12*. All *elegans* sgRNAs for marker genes were taken from Arribere, 2014.

Repair Oligonucleotides (S2)

Repair templates expanded 100 base pairs around the sgRNA to ensure the more efficient short-range HDR was used for repair. Yellow highlighting indicates a mutation of interest and green signifies mutations to destroy the PAM site and create a novel restriction enzyme cut site. All mutations beside the mutation of interest caused silent mutations. *C. elegans* repair oligonucleotides were taken from Arribere, 2014.

Cel-rol-6

TGTGGGTTGATATGGTTAAACTTGGAGCAGGAACCGCTTCCAACCGTGTGCGCTGCCAAC
AATATGGAGGATATGGAGCCACTGGTGTTCAGCCACCAGCACCAAC

- BbvI cut site introduced

Cel-dpy-10

CACTTGAACTTCAATACGGCAAGATGAGAATGACTGGAAACCGTACCGCATGCGGTGCCT
ATGG TAGCGGAGCTTCACATGGCTTCAGACCAACAGCCTAT

- SphI cut site introduced

Cel-sqt-1

GGGGATCCATCAGCATGTGGAGTTGGGGTAGCGTTCGTCTCTTCATATTGGCAGCGGACA
CGTTGCTAGATCTTCCTATAACCACTATGTCCTTCCACAATCC

- BbvI cut site introduced

Cbr-rol-6

GGGTTGATATGGTCAAGCTTGGAGCTGGAACCGCTTCAAACAGAGTGAGATGCCAACAA
TACGGTGGATACGGAGCCAGTGGAGTTCAGCCACCAGCACCA

- XcmI cut site introduced

Cbr-dpy-10

CTCTAGAACTTCAATTCGGCAAAATGAAACTATCCGGAAATCGTACGGCATGCGGTGCTT
ATGGAAGCGGAGCTTCCCATGGATTCAGACCAACTGCTTAT

- SphI cut site introduced

Cbr-sqt-1

GATTGTGGAAGGATATTGTTGTGATTGGAAGAAACAGCAAGCGTGTACGGTGTCAGTAT
GAAGAAACCAACGCCACCCCAACCCCACACGCTGATGGATCC

- HpyCH4III cut site introduced

Cbr-lin-12 constitutive

CAATGCTAAATGCCTATACAAAGACTCTCAAACTGTTGTCGATTTGATCTTCTCAGGACT
TGCCAAGAAAGGAATCAACTCTTTTGGTATCCCGATTTCAG

- DdeI cut site introduced

Cbr-lin-12 l.o.f.
CGGCTCCTACGGTTCATTTTGCGAGAAAAGCTGCCCGTAGACTTTTGATTCCAATCAAAA
ATGTGTCTACAACGAAGAGAATCAAGCAACATTATGTGTT
- BsexI cut site introduced

Verification Primers (S3)
Primers surrounded the mutation of interest and allowed mutation insert to be determined by digests that would cut the experimental but not the wild type. *Elegans* primers were taken from Arribere, 2014.

Cel-rol-6
-5' to 3' forward
GCCATTGTATTTTCTGGAGCCAC
-3' to 5' reverse
CTCCACGTGGTCCTCCTCCATTC
Cut size wild type: 436 bp
Cut size experimental: 235 and 201 bp

Cel-dpy-10
-5' to 3' forward
GTCAGATGATCTACCGGTGTGTCAC
-3' to 5' reverse
GTCTCTCCTGGTGCTCCGTCTTCAC
Cut size wild type: 631 bp
Cut size experimental: 368 and 263 bp

Cel-sqt-1
-5' to 3' forward
GCGTCGCGTCCCTTCTCTCCTG
-3' to 5' reverse
ACATCCGTACTCCTTATCTCCCG
Cut size wild type: 981 bp
Cut size experimental: 491 and 491 bp

Cbr-rol-6
- 5' to 3' forward
GAATGAGCTGGATGCGGAAATCG
-3' to 5' reverse
TTGTGGGCATGTGAAGCAGC
Cut size wild type: 528 bp
Cut size experimental: 373 and 155 bp

Cbr-dpy-10
- 5’ to 3’ forward
TGTTGACAGAGAAATGGCTTATTGC
- 3’ to 5’ reverse
TTTGGAGTGGTTCCTGGCATTC
Cut size wild type: 343 bp
Cut size experimental: 206 and 137 bp

Cbr-sqt-1
- 5’ to 3’ forward
100 GGATTCAGAGAGCAACTCGACAC
- 3’ to 5’ reverse
567 TCCTTGTGGGCAAGTGAAGC
Cut size wild type: 567 bp
Cut size experimental: 432 and 144 bp

Cbr-lin-12 constitutive
- 5' to 3’ forward
CGTGGAAGCCTCTCCAGAATATC
- 3’ to 5’ reverse
GTCCAAACTGGTGCATTGATAATCC
Cut size wild type: 1927 and 385bp
Cut size experimental: 1729, 385, and 198 bp
- 5’ to 3’ forward
GAAATGGATGTGAGAAATTAACAGAAC
- 3’ to 5’ reverse
GTCCAAACTGGTGCATTGATAATCC
Cut size wild type: 366 bp
Cut size experimental: 198 and 169 bp

Cbr-lin-12 l.o.f.
- 5’ to 3’ forward
CCCTTTACTCCAAATTCCCGTCTTC
- 3’ to 5’ reverse
ATTCAATTTCTGCGTTCTACGGTG
Cut size wild type: 791 and 669 bp
Cut size experimental: 791, 410, and 259 bp

The *lin-12* constitutive verification primers had two forward primers: one found about 2 kb back in the gene and one that was much closer to the mutation of interest. These primers were designed to avoid a paralog of *lin-12* in the *briggsae* genome that possesses a near identical sequence. The far primer was specific only to the CBG06829 gene of interest in this experiment while the closer forward primer contained a one base pair difference between CBG06829 and the paralog (indicated by the green highlighted text).

Sequencing Primers (S4)
Elegans primers were taken from Arribere, 2014.

Cel-rol-6 R primer
CCACCTCCTGGGAACTTTGGTTG
Found 82 base pairs downstream from the end of the repair template.

Cel-dpy-10 F primer
TGTCTGTGTTGCTCTCCCAATTATG
Found 124 base pairs upstream from the start of the repair template.

pDD162 R sequencing
CCATTCGCCATTCAGGCTGC
Found 116 base pairs downstream from the expected sgRNA insert site in pDD162.

Cbr-rol-6 primer
CCACCTCCTGGGAACTTTGGTTG
Found 82 base pairs downstream from the end of the repair template.

References

Arribere JA, Bell RT, Fu BX, Artiles KL, Hartman PS, Fire AZ. Efficient marker-free recovery of custom genetic modifications with CRISPR/Cas9 in *Caenorhabditis elegans*. Genetics. 2014;198(3):837–846.

Artavanis-Tsakonas, S., Rand, M.D., and Lake, R.J. (1999). Notch signaling: cell fate control and signal integration in development. Science *284*, 770–776.

Baker NE, Yu S. The EGF receptor defines domains of cell cycle progression and survival to regulate cell number in the developing Drosophila eye. Cell. 2001;104(5):699–708.

Berset T, Hoier EF, Battu G, Canevascini S, Hajnal A. Notch inhibition of RAS signaling through MAP kinase phosphatase LIP-1 during C. elegans vulval development. Science. 2001;291: 1055–1058.

Brenner S. The genetics of *Caenorhabditis elegans*. Genetics 77, 71–94 (1974).

Cong L, Ran FA, Cox D, Lin S, Barretto R, Habib N, Hsu PD, Wu X, Jiang W, Marraffini LA, Zhang F. Multiplex genome engineering using CRISPR/Cas systems. Science. 2013;339:819–823.

Cutter AD. Divergence times in Caenorhabditis and Drosophila inferred from direct estimates of the neutral mutation rate. Molecular Biology and Evolution. 2008;25(4):778–86.

Dawes, A. T., Wu, D., Mahalak, K. K., Zitnik, E. M., Kravtsova, N., Su, H., & Chamberlin, H. M. (2017). A computational model predicts genetic nodes that allow switching between species-specific responses in a conserved signaling network. *Integr. Biol., 9*(2), 156-166.

Dianov GL, Hubscher U. Mammalian base excision repair: the forgotten archangel. Nucleic Acids Res. 2013;41:3483–3490.

Dickinson D. J., Ward J. D., Reiner D. J., Goldstein B., 2013. Engineering the *Caenorhabditis elegans* genome using Cas9-triggered homologous recombination. Nat. Methods 10(10): 1028–1034.

Espinoza I, Miele L. Deadly crosstalk: Notch signaling at the intersection of EMT and cancer stem cells. Cancer Lett. 2013;341(1):41–45.

Félix MA (2012) Evolution in developmental phenotype space. Curr Opin Genet Dev 22: 593–599.

Flores GV, Duan H, Yan H, Nagaraj R, Fu W, Zou Y, et al. Combinatorial signaling in the specification of unique cell fates. Cell. 2000;103(1):75–85.

Galluzzo P, Bocchetta M. Notch signaling in lung cancer. Expert Rev Anticancer Ther. 2011;11(4) 533–540.

Giurumescu CA, Chisholm AD. Cell identification and cell lineage analysis. Meth Cell Biol. 2011;106:325–341.

Greenwald I, Seydoux G. Analysis of gain-of-function mutations of the *lin-12* gene of *Caenorhabditis elegans*. Nature. 1990;346:197–199.

Gupta B.P., Sternberg P.W. The draft genome sequence of the nematode Caenorhabditis briggsae, a companion to *C. elegans*. Genome Biol. 2003;4:238.1-238.4.

Guruharsha K.G., Kankel M.W., Artavanis-Tsakonas S. The Notch signalling system: recent insights into the complexity of a conserved pathway. Nat. Rev. Genet. 2012;13:654–666.

Herman RK, Hedgecock EM. Limitation of the size of the vulval primordium of *Caenorhabditis elegans* by lin-15 expression in surrounding hypodermis. Nature. 1990;348:169–171.

Horvitz H. R., Sternberg P. W., 1991. Multiple intercellular signalling systems control the development of the *Caenorhabditis elegans* vulva. Nature 351: 535–541.

Hsu P.D., Scott D.A., Weinstein J.A., Ran F.A., Konermann S., Agarwala V., Li Y., Fine E.J., Wu X., Shalem O. DNA targeting specificity of RNA-guided Cas9 nucleases. Nat. Biotechnol. 2013;31:827–832.

Jinek, M., Chylinski, K., Fonfara, I., Hauer, M., Doudna, J. A., & Charpentier, E. (2012). A Programmable Dual-RNA-Guided DNA Endonuclease in Adaptive Bacterial Immunity. *Science, 337*(6096), 816-821.

Kane, N. S., Vora, M., Varre, K. J., & Padgett, R. W. (2016). Efficient Screening of CRISPR/Cas9-Induced Events in Drosophila Using a Co-CRISPR Strategy. *G3: Genes|Genomes|Genetics, 7*(1), 87-93.

Kawamura A, Koshida S, Hijikata H, Sakaguchi T, Kondoh H, et al. (2005) Zebrafish Hairy/Enhancer of split protein links FGF signaling to cyclic gene expression in the periodic segmentation of somites. Genes Dev 19 (10) 1156–1161.

Kim H., Ishidate T., Ghanta K. S., Seth M., Conte D., Jr, et al. , 2014. A co-CRISPR strategy for efficient genome editing in *Caenorhabditis elegans*. Genetics 197(4): 1069–1080.

Lambie, E.J., and Kimble, J. (1991). Two homologous regulatory genes, *lin-12* and *glp-1*, have overlapping functions. Development *112*, 231–240.

Ma Y., Zhang L., Huang X. Genome modification by CRISPR/Cas9. FEBS J. 2014;281:5186–5193.

Mello CC, Kramer JM, Stinchcomb D, Ambros V. Efficient gene transfer in *C. elegans*: extrachromosomal maintenance and integration of transforming sequences. Embo J. 1991;10(12):3959–3970.

Paix A., Folkmann A., Rasoloson D., Seydoux G., 2015. High efficiency, homology-directed genome editing in *Caenorhabditis elegans* using CRISPR-Cas9 ribonucleoprotein complexes. Genetics 201(1): 47–54.

Petcherski, A.G., and Kimble, J. (2000). LAG-3 is a putative transcriptional activator in the *C. elegans* Notch pathway. Nature *405*, 364–368.

Rudel D, Kimble J. Evolution of discrete Notch-like receptors from a distant gene duplication in *Caenorhabditis*. Evol Dev. 2002;4:319–33.

Sherwood D.R., Sternberg P.W. Anchor cell invasion into the vulval epithelium in C. elegans. Dev. Cell. 2003;5:21–31.

Wang M, Sternberg PW. Pattern formation during C. elegans vulval induction. Curr Top Dev Biol. 2001;51:189–220.

Yamamoto S., Schulze K.L., Bellen H.J. Introduction to Notch signaling. Methods Mol. Biol. 2014;1187:1–14

Zhang F, Wen Y, Guo X. CRISPR/Cas9 for genome editing: progress, implications and challenges. Hum Mol Genet. 2014;23(R1):R40–6.